

# On-line stator ground-fault location method for synchronous generators based on 100% stator low-frequency injection protection

F.R. Blánquez\*, C.A. Platero, E. Rebollo, F. Blázquez

*Electrical Engineering Department, Universidad Politécnica de Madrid, Spain*



## ARTICLE INFO

### Article history:

Received 22 September 2014

Received in revised form 16 March 2015

Accepted 21 March 2015

### Keywords:

Fault detection

Fault location

Generators

Protection

Rotating machines

Power system protection

## ABSTRACT

Locating stator-winding ground faults accurately is a very difficult task, especially in high-impedance grounded generators. Through the conventional measurements of power plants, obtaining the precise location of these defects in on-line operating conditions is not possible, because the fault resistance is unknown. This paper presents a general algorithm for locating stator-winding ground faults in on-line operating conditions, based on the measurements provided by the 100% ground-fault low-frequency injection protection, and other available measurements. Some simplifications are applied to the general algorithm, and a simplified method is also presented for generators with especially low capacitance-to-ground, whose implementation in modern protective relays is more simple. The location through the general algorithm, and the simplified algorithms, has been validated by simulation and experimental tests, for several fault resistance values at different points of the stator winding. These algorithms assure an acceptable accuracy for a wide range of fault resistance values and locations, without the need of any additional equipment.

© 2015 Elsevier B.V. All rights reserved.

## 1. Introduction

Electrical protections are currently a primary concern not only for maintaining the reliability of the power system, but also for assuring the safe operation under faulty conditions. In power plants, protective systems are vital for guaranteeing the safety of the personnel and for minimizing the damage on the power components and equipment during any type of events.

One of the most common defects of power synchronous generators is the stator-winding ground fault [1]. The consequences of this type of faults entirely depend on the generator grounding scheme [2]. If the generator is grounded through a low impedance, the fault current may be very high [3]. In this type of grounding scheme the damage caused by a solid ground fault at the generator terminal could be very severe, since the stator winding is solidly short-circuited [4]. The defect in this case is easy to locate because the damage caused by the defect is visible.

On the other hand, medium and large sized synchronous generators are grounded through a high impedance, whose value is generally set in order to limit the neutral current. In case of solid ground-fault at the generator terminal, this current is typically limited to 5 A or 10 A [5]. This limits the damage in the stator

winding, nevertheless it makes the fault location less visible, even if the rotor is extracted.

The most basic stator ground-fault protection scheme is based on the measurement of the neutral voltage (59N) [6] or the neutral current (51N). Since stator ground faults cause the appearance of a neutral circulating current (and therefore a neutral voltage), any ground fault may be detected by the measurement of any of these variables [7]. However, the setting of the trip threshold to zero is not recommended for this scheme, since the presence of any transient neutral current may cause an unwanted trip command. This kind of protection scheme is generally called “95% stator ground-fault protection”, attributable to the portion of the stator winding that they protect.

For the protection of the remaining 5% of the stator winding, any of the “100% stator ground-fault protection” schemes are used [8,9]. One of the most extended schemes is based on the measurement of the third-harmonic component of the neutral voltage (27NTH) [10]. The magnitude of this component depends mainly on the value of the capacitance-to-ground of the generator stator winding and other components such as the generator breaker or the step-up transformer. However, the third-harmonic component also depends on the operating conditions of the generator [11,12]. According to this, the operation of 27NTH is normally blocked during the start-up process, as well as during low active or reactive power operating conditions [5], in order to avoid unwanted trip commands.

\* Corresponding author. Tel.: +34 619266508.  
E-mail address: [fr.blanquez@gmail.com](mailto:fr.blanquez@gmail.com) (F.R. Blánquez).

As a consequence of this limitation, another extended solution is the low-frequency injection scheme (64S). It is based on the injection of a low-frequency voltage signal (typically 12.5 Hz, 15 Hz or 20 Hz) in the grounding impedance through a band-pass filter. This protection obtains the equivalent impedance by measuring the low-frequency current, which changes during ground faults. Although this scheme is expensive, it is becoming extensively used, since it is able to be kept enabled when the machine is off-line [5]. This protection scheme is becoming a very active research topic [13–15], mainly because there are no unwanted trips through this scheme. An additional feature of this protection is the accurate measurement of the equivalent resistance, from which the fault-resistance value can be obtained.

Nowadays, after the detection of a ground fault, the generating unit is removed from service. Once the insulation level is checked, and the existence of the ground fault is confirmed, the complete rotor has to be extracted just for location purposes. Then, the ground fault has to be located. This operation may become really difficult, especially in high-impedance grounded generators, in which the maximum neutral current is limited up to 10 A. This low fault current does not damage the stator core, and it makes impossible the visual location of the insulation failure. Then, the fault is located by using different methods. Some technicians inject high-value current through the faulty winding and the iron core in order to visually detect the fault. This high current could damage the iron lamination insulation. Other methods of fault location include non-damaging techniques, which consist of dividing the stator winding into two parts and checking the insulation level of each one. Thereafter, the part of the winding with low level of insulation is again divided into two parts, and both of them are checked again. In this way, through the division of the stator winding in several parts, the ground fault can be located. This process of the location and repair of the fault can take several days and it is quite expensive. If some information about the location of the fault was provided, the time of the repair would be reduced drastically. On the other hand, in some particular cases the ground fault is even more difficult to locate, due to the insulation failure being present only at rated voltage of the winding. Then, the fault location would have to be obtained by the use of high voltage tests.

Although the detection of the stator ground faults is extensively studied [16–20] and solved, the location of the defect along the field winding is currently being addressed in many contributions, not only for large synchronous generators [21,22], but also for other types of electrical machines, such as wind generators [23]. In this paper, an algorithm for on-line location of ground faults in generators with low-frequency 100% stator and 95% ground-fault protections is proposed. Firstly, the measurements of the neutral voltage and current (95% ground-fault protection) are evaluated as a fault locator (Simplified Method “A”) in Section 2 which provides unacceptable results. Secondly, In Section 3, a high-accurate location method is proposed. It uses the equivalent resistance provided by the 100% ground fault low-frequency injection protection,

the neutral current (or the voltage) and the system parameters, to obtain the fault resistance value, and thus the location of the fault. Finally, some simplifications are applied to the general algorithm in order to obtain Simplified Method “B”, which is applicable to synchronous generators with especially low capacitance-to-ground. The implementation of this simplified method in protective relays would be easier. These methods have been evaluated by simulation and experimental tests, and the results are described in Sections 4 and 5, respectively. By the use of the novel on-line location method presented in this paper, modern protective systems may be able to provide both the value of the fault resistance and the location of the ground fault during the trip, which will make possible detecting isolation failures that only appears with the generator at rated voltage and will drastically reduce the repair time after the rotor extraction.

## 2. Theoretical approach of ground-fault location in stator windings

In synchronous generators grounded through a high-value impedance, the stator ground-faults are generally detected by using a neutral overvoltage protection (59N), or neutral overcurrent protection (51N). In some cases, this protection is installed together with a 100% ground-fault protection scheme, which covers 5–10% of the stator winding that is closer to the neutral point. In Fig. 1, the simplified scheme of a power plant is shown, where the general scheme of 59N is represented. In this figure, a ground-fault is represented in phase A, where  $R_f$  is the fault resistance,  $I_f$  is the fault current,  $U_n$  is the generator phase voltage, and  $x$  represents the exact location of the ground fault, from 0 pu or 0% (Neutral, N) to 1 pu or 100% (Terminal, A). This ground fault causes the appearance of a neutral voltage ( $V_N$ ), and a circulating neutral current ( $I_N$ ), measured by the previously described protections. In large size generators, several capacitances-to-ground have to be taken into account, such as the equivalent capacitance-to-ground of the stator winding ( $C_g$ ), and  $C_z$ , which includes the capacitance-to-ground of the generator breaker, the generator step-up (GSU) transformer, the auxiliary transformer and the bus bars, among others.

In power plants, the measurements of this scheme (Fig. 1) which can be obtained are  $I_N$ ,  $V_N$ ,  $U_n$ , and the terminal voltage ( $V_A$ ).  $R_N$  is the grounding resistance, which is represented in the primary winding of the grounding transformer, although the installation of this resistance in the secondary winding is also common. The value of  $R_N$  is typically obtained as the resistance necessary to limit the neutral current to 10 A (5 A is also used), in case of a solid ground-fault at the generator terminal. According to this, a ground fault is detected when the value of  $I_N$  is higher than the 51N setting threshold (whose value is generally set to 5% of 10 A), or when the value of  $V_N$  is higher than the 59N setting threshold (whose value is generally set to 5% of  $U_n$ ). In both cases, the upper 95% of the stator winding is protected. Lower setting levels are not recommended because of the possibility of unwanted trip commands [1].

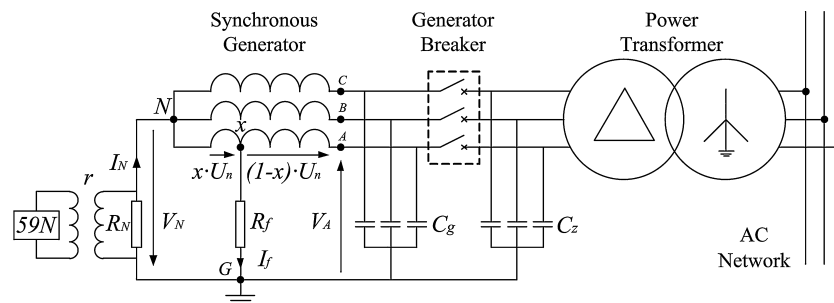


**Fig. 1.** Simplified scheme of a power plant with a synchronous generator grounded through a high-value resistance equipped with 95% ground-fault protection (59N).

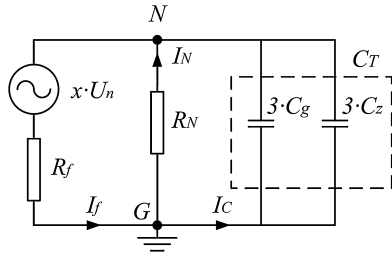


**Fig. 2.** Equivalent circuit of the fundamental frequency grounding network for zero sequence component.

The equivalent circuit of the grounding network for zero sequence component, in case of ground-fault, is shown in Fig. 2 [3], where  $C_T$  represents the total capacitance of the power system (1). This circuit includes only a source with a value of  $x \cdot U_n$  since this is the only one that contributes to the appearance of the zero-sequence voltage in the grounding resistor.

$$C_T = 3 \cdot (C_g + C_z) \quad (1)$$

In this circuit, the parameters  $x$  and  $R_f$  are unknown, however  $I_f$  [3] can be expressed by (2).

$$I_f = \underline{U}_n \cdot x \cdot \frac{1 + j\omega C_T R_N}{R_f(1 + j\omega C_T R_N) + R_N} \quad (2)$$

Since  $I_N$  is measured (3),

$$\underline{I}_N = \frac{1}{1 + j\omega C_T R_N} \cdot \underline{U}_n \cdot x \cdot \frac{1 + j\omega C_T R_N}{R_f(1 + j\omega C_T R_N) + R_N} \quad (3)$$

(2) can be expressed as (4),

$$x \cdot \underline{U}_n = I_N(R_N + R_f(1 + j\omega C_T R_N)) \quad (4)$$

where the underlining denotes phasor,  $\omega$  is the angular frequency (5), and  $f$  is the fundamental frequency (50 Hz or 60 Hz).

$$\omega = 2 \cdot \pi \cdot f \quad (5)$$

The expression (4) provides the relation between  $x$ ,  $R_f$  and  $I_N$  (or  $V_N$ ). As the value of  $R_f$  is unknown, the fault location ( $x$ ) is also unknown. However, some information related to the fault location can be extracted.

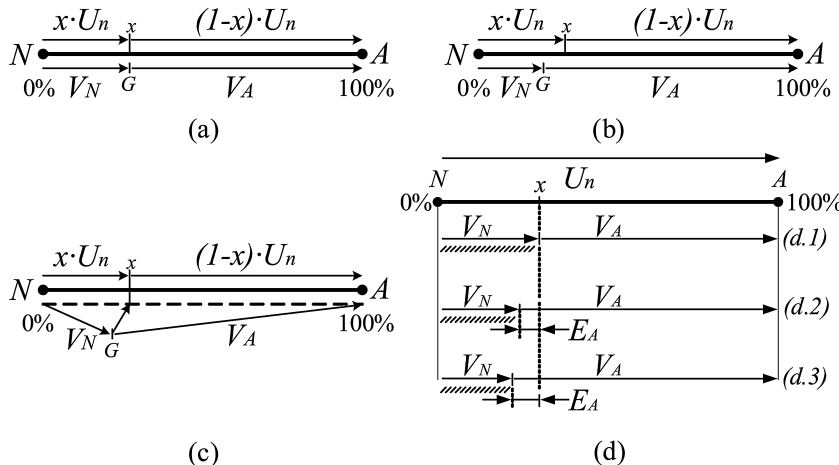


**Fig. 3.** Vector representation of the voltages of the system in case of (a)  $C_T = 0$  and  $R_f = 0$ ; (b)  $C_T = 0$ , and  $R_f \neq 0$ ; (c)  $C_T \neq 0$ , and  $R_f \neq 0$ . (d) Representation of the amplitude of the neutral voltage and terminal voltage: (d.1) with  $C_T = 0$ , and  $R_f = 0$ ; (d.2) with  $C_T = 0$ , and  $R_f \neq 0$ ; (d.3) considering the effect of  $C_T$  and with  $R_f \neq 0$ .

## 2.1. Simplified Method "A" (59N) for ground-fault location in stator windings

Firstly, let's consider the capacitive current ( $I_C$ ) negligible, which means there is no capacitance to ground. This fact is very close to being realistic for small generating units and generators with especially low value of  $C_T$ , as it will be described later. This consideration leads to expression (6).

$$x \cdot U_n \approx I_N(R_N + R_f) \quad (6)$$

Secondly, in case of a solid ground fault ( $R_f = 0$ ), the fault location can be directly obtained as the ratio between  $V_N$  and  $U_n$  (7) (see Fig. 3(a) and (d.1))

$$x_A^* = \frac{I_N \cdot R_N}{U_n} = \frac{V_N}{U_n} \quad (7)$$

where  $x_A^*$  is the first location of the ground-fault by only using the information from 59N or 51N. As the value of the fault resistance increases, this location becomes imprecise (see Fig. 3(b) and (d.2), where  $E_A$  (8) is the total error of this simplified method). Moreover, if value of the capacitance-to-ground is not negligible, the use of this ratio as the fault location is more inaccurate (see Fig. 3(c) and (d.3)).

$$E_A = x - x_A^* = x \cdot \left( 1 - \frac{R_N}{\sqrt{(R_N + R_f)^2 + (\omega C_T R_N R_f)^2}} \right) \quad (8)$$

This error is analyzed in detailed in [24], where it is described that the error of neglecting the fault resistance value is considerably higher than the value of neglecting the capacitance-to-ground for certain values.

Besides the fact that this first location is not acceptable for high values of fault resistance, it may nonetheless be used only for the location of solid ground-fault. Unfortunately, the main problem is that the value of the fault resistance in on-line operating conditions is unknown, only with the information provided by 59N, making this location unreliable. However, expression (4) provides relevant information because, in case of having a way of obtaining the value of  $R_f$ , the value of  $x$  may be also calculated more accurately.

## 3. Algorithm for the stator ground-fault location using 59N+64S

This new location algorithm need the measurement provided by the protection 64S, therefore it can be applied to large synchronous

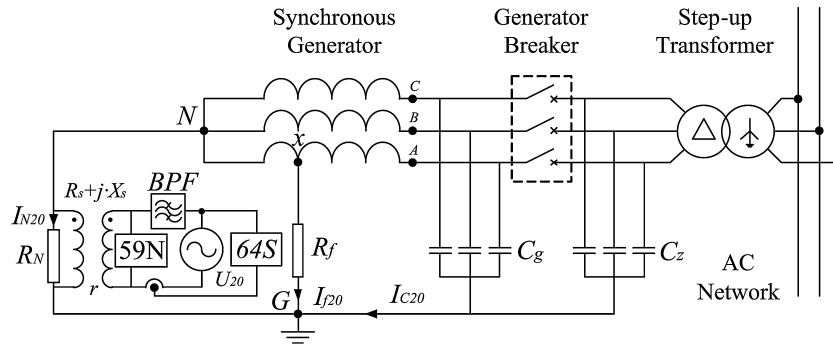


**Fig. 4.** Simplified scheme of a power plant with a synchronous generator grounded through a high-value resistance and low-frequency injection protection scheme.

generators, in which the protection 64S is applicable. For this size of generators, it is a typical practice to have YNd step-up transformers. Nevertheless, this new algorithm is applicable also for systems with YNy or Yy transformers. For low-power synchronous generators, the protection 64S is not generally installed, and without it this location algorithm cannot be implemented.

In Fig. 4, a general scheme of the 100% ground-fault protection, based on low-frequency injection (64S), is shown. This protection scheme is based on the evaluation of the impedance at 20 Hz, obtained using a 20 Hz voltage source,  $U_{20}$ , and a band-pass filter (BPF). The injection is performed in the secondary winding of the grounding transformer, whose ratio is  $r$ . The impedance is obtained using both the low frequency voltage and current registered by the relay (64S). When a ground fault occurs the impedance decreases, and its value depends mainly on the fault resistance. If the value of the impedance goes under the setting threshold (typically 1–2 k $\Omega$ ), this protection function gives a trip command.

In the described scheme,  $R_s$  is the series resistance, which includes the series resistance of the grounding transformer and the connection wires.  $X_s$  is the series reactance, which has also a low influence in the impedance calculation. The effect of both variables can be compensated in the commercial protection devices. The equivalent circuit of the grounding network for low frequency is shown in Fig. 5. As observed, in the case of a ground-fault, the low-frequency source branch ( $U_{20}$ ),  $R_N$  and  $C_T$  are connected in parallel to the faulty branch ( $R_f$ ).

Through this circuit, the low-frequency equivalent impedance is obtained by (9)

$$Z_{20} = R_s + jX_s + \frac{R_N \cdot R_f}{R_N + R_f + j\omega_{20} R_f R_N C_T} \quad (9)$$

where  $\omega_{20}$  is defined by using  $f=20$  Hz (although 12.5 Hz and 25 Hz are also used). As observed, the fault location  $x$  has no influence in this expression, since the value of the stator resistance and inductance is very low. In fact, these parameters are not compensated in commercial relays. This fact makes this relay to detect a ground-fault accurately at any point of the field winding, including the first 5%, for which this protection is intended.

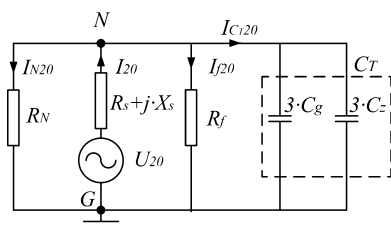


**Fig. 5.** Equivalent circuit of the low-frequency grounding network.

### 3.1. General non-simplified method of ground-fault location in stator windings (59N + 64S)

The expression (9) shows the dependence of this low-frequency impedance on  $R_f$ , and therefore this relation is used as a way for obtaining this variable. Hence, Eqs. (4) and (9) can be used for obtaining the value of  $R_f$  and the fault location ( $x$ ). The solution of Eqs. (10) and (11), which are expressed in magnitude, provides the most accurate value of the fault resistance and location.

$$x \cdot \frac{U_n}{I_N} = |R_N + R_f(1 + j\omega C_T R_N)| \quad (10)$$

$$Z_{20} = \left| R_s + jX_s + \frac{R_N \cdot R_f}{R_N + R_f + j\omega_{20} R_f \cdot R_N \cdot C_T} \right| \quad (11)$$

The value of the fault resistance is obtained by expression (11). Firstly, the real part of the complex impedance  $Z_{20}$  is expressed as (12)

$$R_{20} = R_s + \frac{R_N^2 \cdot R_f + R_N \cdot R_f^2}{(R_N + R_f)^2 + (\omega_{20} R_N R_f C_T)^2} \quad (12)$$

where the resistive part of the low-frequency impedance,  $R_{20}$ , is provided by the actual measurement of the low-frequency protective relay. This expression leads to (13), where only the solution which uses the negative sign is useful.

$$R_f^2 \cdot (R_{20c} \cdot (1 + \omega^2 R_N^2 C_T^2) - R_N) + R_f \cdot (2R_N R_{20c} - R_N^2) + R_N^2 \cdot R_{20c} = 0 \quad (13)$$

From this expression, the value of the fault resistance is obtained as (14)

$$R_f^* = \frac{R_N^2 - 2R_N R_{20c} - \sqrt{R_N^4 \cdot (1 - 4R_{20c}^2 \omega_{20}^2 C_T^2)}}{2R_{20c}(1 + R_N^2 \omega_{20}^2 C_T^2) - 2R_N} \quad (14)$$

where  $R_{20c}$  is the resistive part of the impedance, compensated by the series resistance (15).

$$R_{20c} = R_{20} - R_s \quad (15)$$

Expression (14) allows obtaining the value of the fault resistance without any additional equipment. However, this variable can also be obtained by other proposed methods, that also use the low-frequency injection scheme, but which need the installation of an extra inductance [25].

The calculation of the fault resistance value  $R_f^*$  is used for the fault location, by the expression (10), which can be expressed as (16).

$$x^* = \frac{V_N}{U_n \cdot R_N} \cdot \sqrt{(R_N + R_f^*)^2 + (\omega C_T R_N R_f^*)^2} \quad (16)$$

This general algorithm is the non-simplified location method, which implies that the only error in the location (17) is a consequence of the measurement equipment accuracy, such as the

voltage transformers, current transformers and low-frequency injection source, among others. Hence, this error should be very close to zero.

$$E = x - x^* \approx 0 \quad (17)$$

### 3.2. Simplified Method “B” (59N + 64S) for ground-fault location in stator windings

With the aim of obtaining a simple expression which calculates the ground-fault location, the relations (10) and (11) are simplified. This simplified method would be applicable to generators with a value of capacitance-to-ground particularly low, and its implementation in protective relays would be more simple.

On the one hand, expression (4) is simplified. As described in Section 2, Eq. (4) relates the ground-fault location ( $x$ ) to the fault resistance ( $R_f$ ). In this expression, the fact of considering the capacitive component as negligible affects the accuracy of the relation. However, its effect depends fundamentally on the capacitance value and the generator rated voltage. Neglecting the effect of the capacitance to ground implies considering the magnitude of  $I_f$  as the magnitude of  $I_N$  (see Fig. 2).

If this approximation is considered, Eq. (4) can be expressed as (18)

$$x_B^* \cdot U_n = I_N(R_N + R_{fb}^*) \quad (18)$$

where  $x_B^*$  and  $R_{fb}^*$  represent the calculation of the location of the ground-fault and the calculation of the fault resistance, respectively.

On the other hand, some simplification is also applied to (11), again based on considering as negligible the total capacitance-to-ground. For this low-frequency network the effect of the capacitive component is even lower, given that the frequency is 20 Hz.

Through these considerations, the resistive part of  $Z_{20}$  is expressed as (19)

$$R_{20} = R_s + \frac{R_{fb}^* \cdot R_N}{R_{fb}^* + R_N} \quad (19)$$

Neglecting the effect of the capacitance-to-ground, implies considering the magnitude of  $I_{20}$  as the addition of the magnitude of  $I_{N20}$  and  $I_{P20}$  (see Fig. 5), which implies a very small error for a wide range of values of  $C_T$  for this frequency value.

The expressions (18) and (19) represent the main equations of this simplified algorithm of fault location. By operating both relations, the location of the fault by this method ( $x_B^*$ ) is stated as in (20), which can be expressed as a function of the neutral current or the neutral voltage.

$$x_B^* = \frac{I_N}{U_n} \cdot \frac{R_N^2}{R_N - R_{20c}} = \frac{V_N}{U_n} \cdot \frac{R_N}{R_N - R_{20c}} \quad (20)$$

Finally, the estimation of the fault resistance value ( $R_{fb}^*$ ) can also be obtained as (21).

$$R_{fb}^* = \frac{R_N \cdot R_{20c}}{R_N - R_{20c}} \quad (21)$$

The simplifications applied Eqs. (10) and (11) to obtain the “Simplified Method B” imply an error in the location of the defect. Both the location error added by neglecting the capacitance to ground in expression (4), and the location error added by obtaining  $R_{fb}^*$  through expression (21) are included in  $E_B$  (22).

$$E_B = x - x_B^* = x \cdot \left( 1 - \frac{R_N^2 / (R_N - R_{20c})}{\sqrt{(R_N + R_f)^2 + (\omega C_T R_N R_f)^2}} \right) \quad (22)$$

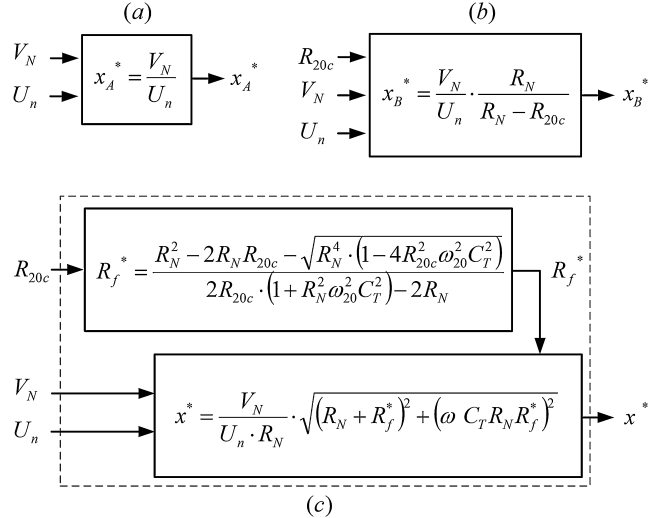


**Fig. 6.** Block diagram of: (a) Simplified Method “A”; (b) Simplified Method “B” and (c) general non-simplified algorithm.

As a summary, the block diagram of the Simplified Methods “A” and “B”, and of the general non-simplified location algorithm are shown in Fig. 6.

## 4. Results of the simulation of stator ground-fault location

This location algorithm has been studied using the realistic 500 MVA power-plant data summarized in Table A.1, and simulated through Matlab. Firstly, in Fig. 7, the results of application of Simplified Method “A”, for  $x \in [0, 100]\%$ , and  $R_f \in [0, 1000]\Omega$ , are represented. The fault location obtained by  $x_A^*$  is shown for  $C_T = 0.5 \mu F$  (Fig. 7(a)) and  $C_T = 2 \mu F$  (Fig. 7(b)). As observed, as  $R_f$  increases, the value of  $x_A^*$  lowers at each case. For instance, if considering  $x = 100\%$  and  $R_f = 1000 \Omega$ , the value of  $x_A^*$  is under 60% in both cases, really far from the fault location expected (100%). In Fig. 7(c) and (d), the error  $E_A$  is represented for the same values of  $C_T$ . It can be noted that, although the value of  $C_T$  decreases from  $2 \mu F$  to  $0.5 \mu F$ , the error  $E_A$  decreases very little. This means that the effect of neglecting  $C_T$  affects considerably less than the fact of neglecting  $R_f$ , which is what mainly makes this simplified method inaccurate. For instance, if considering again  $x = 100\%$  and  $R_f = 1000 \Omega$ , the error  $E_A$  remains in both cases over 45%, which is unacceptable. In conclusion, the fault location by  $x_A^*$  is accurate only if the fault resistance value is close to zero, as expected.

The results of the location of stator ground-fault through the Simplified Method “B” ( $x_B^*$ ), are shown in Fig. 8(a) (for  $C_T = 0.5 \mu F$ ) and in Fig. 8(b) (for  $C_T = 2 \mu F$ ). In both cases, the location profile (from  $x = 0$  to  $x = 100\%$ ) for any fixed  $R_f$  can be compared with the location profile for  $R_f = 0$ , in which the location is more accurate. The similarity of these profiles shows the improvement of the results by using this location algorithm. In the concrete case of  $C_T = 2 \mu F$  the improvement of the location can be clearly observed if comparing Fig. 8(b) to Fig. 7(b). The location error obtained by applying Simplified Method “B” is shown in Fig. 8(c) and (d) for the same values of  $C_T$  as previously. As observed,  $E_B$  remains under 7% in any condition for  $C_T = 2 \mu F$ , and it decreases considerably when the value of  $C_T$  decreases to  $0.5 \mu F$  ( $E_B$  remains under 0.5% for any case). In conclusion, the effect of neglecting the value of  $C_T$  affects to the error  $E_B$ , making it lower as the value of  $C_T$  decreases.

The results of the general non-simplified algorithm are not represented or shown since the fault location is perfect by simulations, and there is no error. However, an additional aspect has to be pointed out. Some error in the fault location by the general

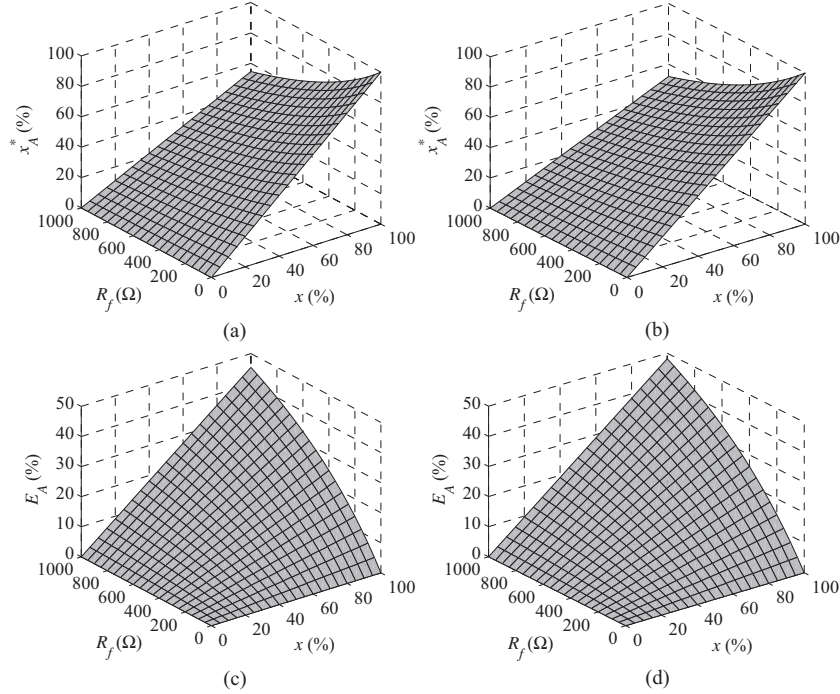


**Fig. 7.** Results of application of the Simplified Method “A” (59N).  $x_A^*$  (a) and  $E_A$  (b) for  $C_T = 0.5 \mu\text{F}$ ;  $x_A^*$  (c) and  $E_A$  (d) for  $C_T = 2 \mu\text{F}$ .

non-simplified algorithm may appear as a consequence of an imprecise measurement of the capacitance value or of the neutral voltage.

The value of the total capacitance-to-ground can be obtained in field during the commissioning. However, although the value of capacitance-to-ground can be obtained by high-accurate equipment, which assures a precise measurement, the error introduced in the algorithm by a wrong setting of the value of this capacitance may cause error in the final location (see Fig. 9(a)). The error of

considering the total capacitance-to-ground as zero, is exactly the error provided by Simplified Method “B” ( $E_B$ ), and any error caused by considering this capacitance lower than the real value will be smaller than  $E_B$ .

On the other hand, a measurement error of the VT, or a bad setting of the VT ratio in the protective system, may cause again errors in the location provided by the algorithm (see Fig. 9(b)). Both described errors can be perfectly avoided during the commissioning.

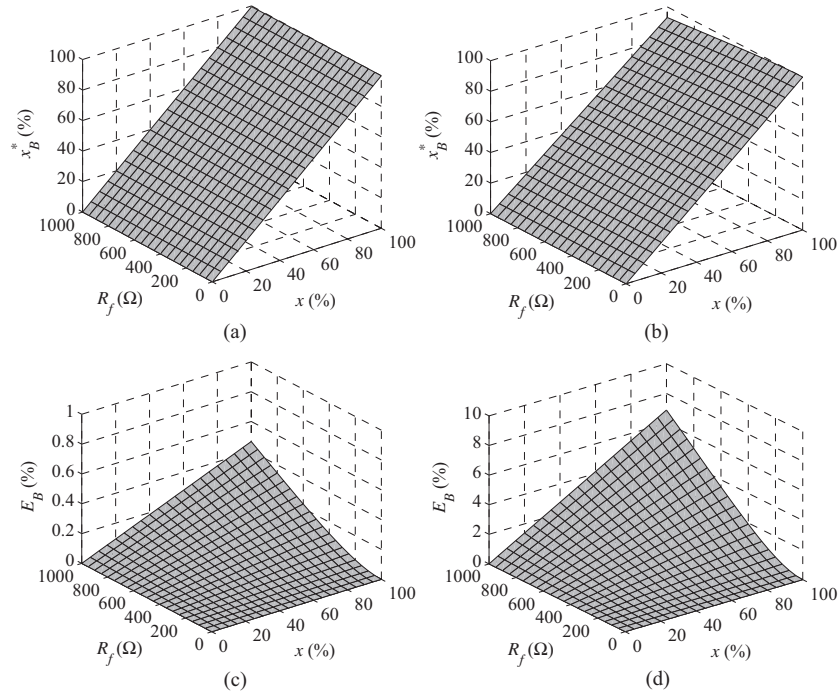


**Fig. 8.** Results of application of the Simplified Method “B” (59N + 64S).  $x_B^*$  (a) and  $E_B$  (b) for  $C_T = 0.5 \mu\text{F}$ ;  $x_B^*$  (c) and  $E_B$  (d) for  $C_T = 2 \mu\text{F}$ .

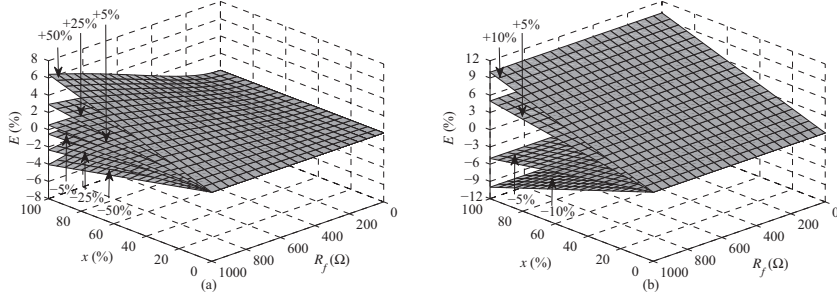


**Fig. 9.** Error obtained by general non-simplified location algorithm (59N+64S) due to (a) error in the input value of capacitance-to-ground in the algorithm  $\pm 5\%$ ,  $\pm 25\%$ ,  $\pm 50\%$ ; (b) error in the neutral voltage measurement ( $V_N$ )  $\pm 5\%$ ,  $\pm 10\%$ ;  $C_T = 2 \mu F$ .

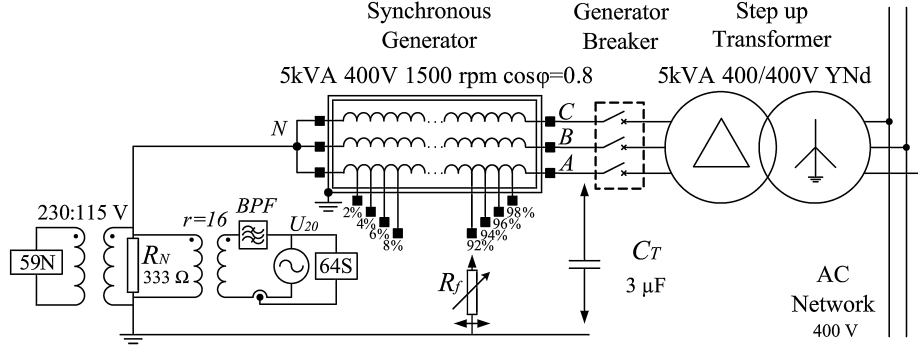


**Fig. 10.** Laboratory 5 kVA experimental setup simplified diagram.

## 5. Laboratory tests and results

The tests have been carried out in a laboratory set-up, whose simplified scheme is shown in Fig. 10. The 5 kVA synchronous generator is especially designed to perform stator ground faults, as some internal points of a phase of the stator winding are accessible (2%, 4%, 6%, 8%, 92%, 94%, 96% and 98%). An additional capacitance-to-ground has been added in order to make the experimental tests more representative (3  $\mu F$ ). The laboratory platform has both the same commercial protective relays and 100% ground fault low-frequency injection protection as a large-size synchronous generator. The technical data of this experimental setup is summarized in Table A.2 of the Appendix. In Fig. 11, a picture of the experimental setup is shown, where all the components can be identified.

Firstly, the ground-fault location by Simplified Method “A” is evaluated. The values of  $x_A^*$  and  $E_A$  expected by equations are represented in Figs. 12(a) and 13(a), respectively. The values of  $x_A^*$  obtained and the error  $E_A$  obtained in laboratory tests are represented in Figs. 12(b) and 13(b), respectively. As observed, the experimental and expected results are very similar. However, as it was expected, the location error in the upper part of the winding is higher than 75%, this being unacceptable. Secondly, the values of the fault location obtained by the Simplified Method “B”,  $x_B^*$ , are shown in Fig. 14(a) (simulation) and Fig. 14(b) (experimental). Again, the experimental and the expected results are very similar. The errors in the fault location are represented in Fig. 15, where once again the expected results and the experimental results can be compared. As observed, the location error is reduced below 5% in all the tests.

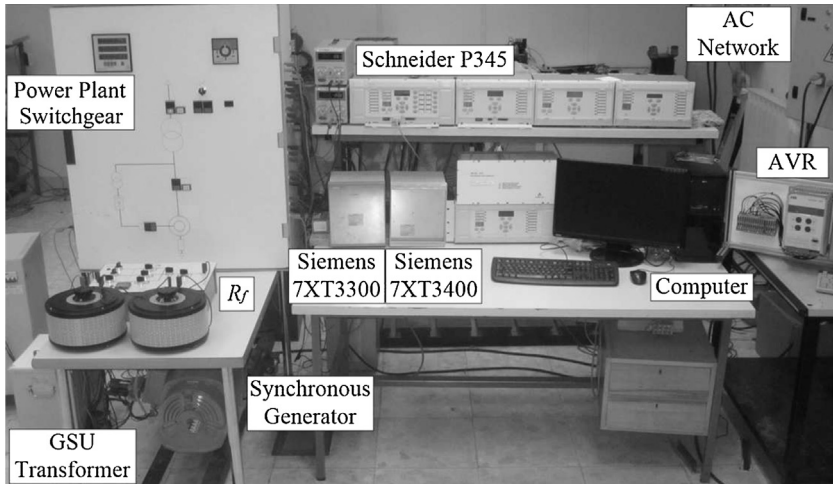


**Fig. 11.** Laboratory 5 kVA experimental setup.

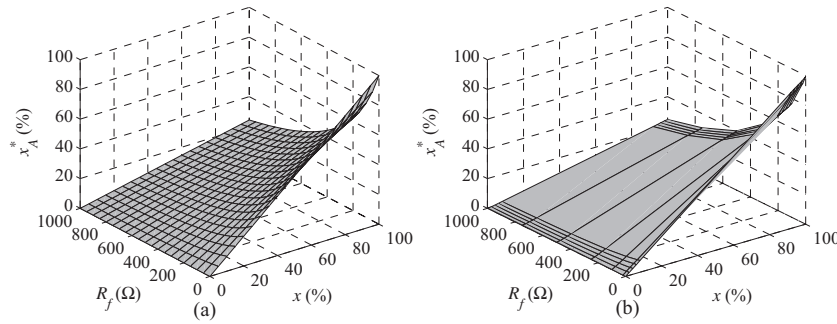


**Fig. 12.** Simplified Method “A” (59N). Fault location estimation by  $x_A^*$ . (a) Simulation and (b) experimental.

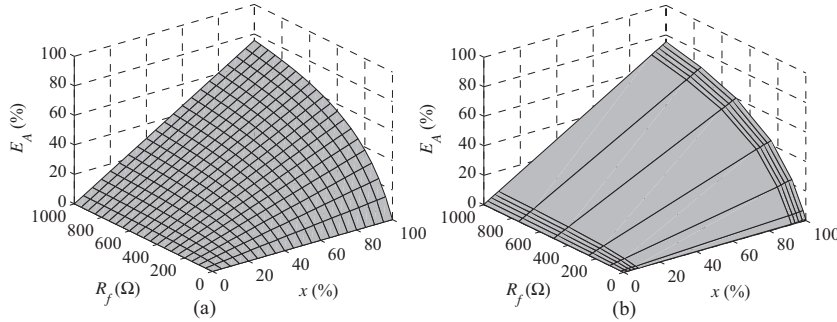


**Fig. 13.** Simplified Method “A” (59N). Fault location error  $E_A$ . (a) Simulation and (b) experimental.

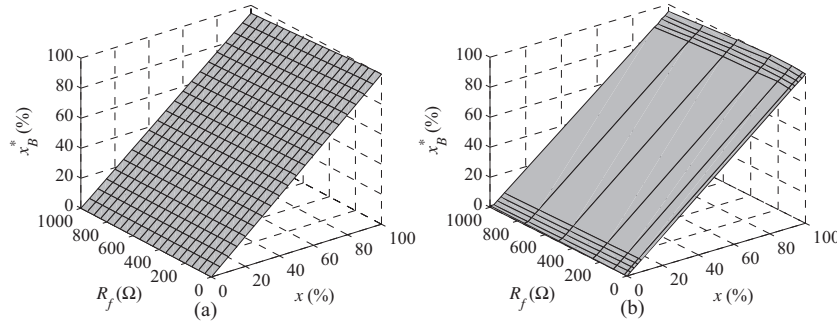


**Fig. 14.** Simplified Method “B” (59N + 64S). Fault location estimation,  $x_B^*$ . (a) Simulation and (b) experimental.

Finally, the results of fault location by the general non-simplified location algorithm is shown in Fig. 16, where the similarity between the experimental and expected results can be observed. The error of fault location by the general non-simplified location algorithm are represented in Fig. 17. As described, by this location algorithm the only error expected is a consequence of the measurement equipment accuracy. Therefore, error  $E$  is expected to be close to zero. As

observed in the aforementioned figure this location error remains under 2%, which is considered as acceptable.

In order to compare the results of the fault location, the numerical value of the variables is summarized in Tables 1–3. The results of stator ground faults in the described taps for  $R_f = 100 \Omega$  (Table 1) and for  $R_f = 1000 \Omega$  (Table 2), come to show two important aspects. Firstly, the error by the location estimation by measurements of

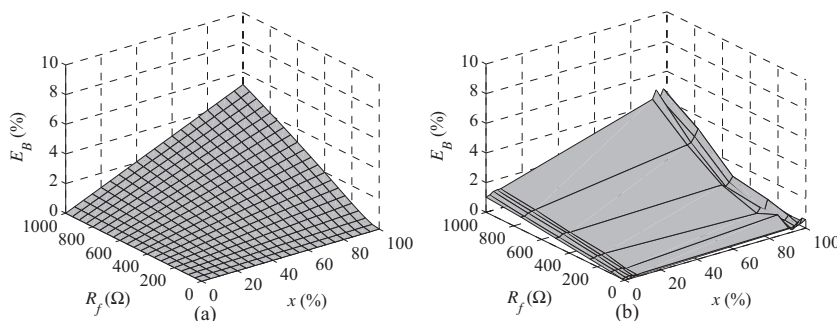


**Fig. 15.** Simplified Method “B” (59N + 64S). Fault location error  $E_B$ . (a) Simulation and (b) experimental.

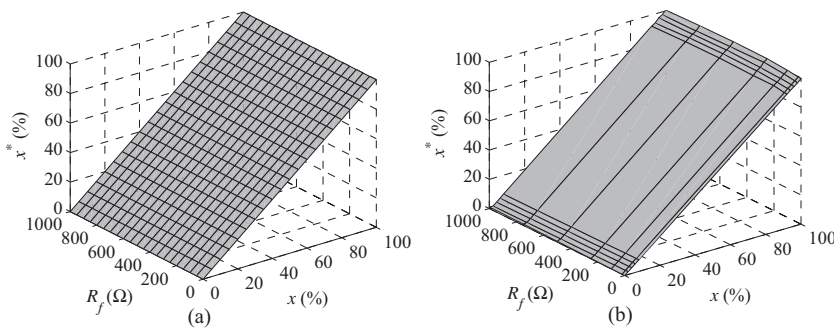


**Fig. 16.** General non-simplified location algorithm (59N + 64S). Fault location estimation,  $x^*$ . (a) Simulation and (b) experimental.

**Table 1**

Results of location of ground-fault and location error for  $R_f = 100 \Omega$  (experimental test).

$x$ (%)	$V_N$ (A)	$R_{20c}$ ( $\Omega$ )	$x_A^*$ ( $E_A$ ) (%)	$x_B^*$ ( $E_B$ ) (%)	$x^*$ ( $E$ ) (%)
0	0.2	78.3	0.08 (-0.08)	0.11 (-0.11)	0.11 (-0.11)
2	3.3	78.3	1.43 (0.57)	1.86 (0.14)	1.87 (0.13)
4	6.8	78.2	2.96 (1.04)	3.87 (0.13)	3.88 (0.12)
6	10.3	78.3	4.47 (1.53)	5.84 (0.16)	5.86 (0.14)
8	13.9	78.4	6.06 (1.94)	7.93 (0.07)	7.95 (0.05)
92	163.3	78.0	71.00 (21.00)	92.73 (-0.73)	93.01 (-1.01)
94	166.3	77.8	72.30 (21.70)	94.34 (-0.34)	94.62 (-0.62)
96	169.5	78.0	73.68 (22.32)	96.22 (-0.22)	96.51 (-0.51)
98	172.6	79.2	75.06 (22.94)	98.47 (-0.47)	98.78 (-0.78)
100	176.7	78.0	76.83 (23.17)	100.32 (-0.32)	100.62 (-0.62)

**Table 2**

Results of location of ground-fault and location error for  $R_f = 1000 \Omega$  (experimental test).

$x$ (%)	$V_N$ (A)	$R_{20c}$ ( $\Omega$ )	$x_A^*$ ( $E_A$ ) (%)	$x_B^*$ ( $E_B$ ) (%)	$x^*$ ( $E$ ) (%)
0	0.6	246.8	0.26 (-0.26)	1.02 (-1.02)	1.08 (-1.08)
2	0.5	246.9	0.24 (1.76)	0.91 (1.09)	0.96 (1.04)
4	1.6	246.9	0.71 (3.29)	2.74 (1.26)	2.89 (1.11)
6	2.8	246.8	1.22 (4.78)	4.70 (1.30)	4.96 (1.04)
8	4.0	247.2	1.73 (6.27)	6.70 (1.30)	7.07 (0.93)
92	52.2	246.8	22.69 (69.31)	87.61 (4.39)	92.31 (-0.31)
94	53.1	246.7	23.07 (70.93)	89.06 (4.94)	93.85 (0.15)
96	54.5	246.9	23.69 (72.31)	91.67 (4.33)	96.61 (-0.61)
98	55.6	246.5	24.18 (73.82)	93.13 (4.87)	98.12 (-0.12)
100	56.7	246.9	24.66 (75.34)	95.40 (4.60)	100.54 (-0.54)

the 95% ground-fault protection scheme (Simplified Method "A") is very high, making it unacceptable. Secondly, the Simplified Method "B" provides an acceptable accuracy for every case ( $E_B$  is always under 5%) in both cases of fault-resistance value. As expected, the best accuracy is obtained in faults closer to the neutral point, so that the error  $E_B$  rises as the fault location gets closer to the generator terminal. Finally, the general non-simplified method provides the

best accuracy in the whole range of fault locations, for both values of fault resistance, as expected.

In order to observe the effect of the fault resistance value, more results are summarized in Table 3, where the location estimation in the 8% and the 92% of the winding are shown for several values of fault resistance. As expected, in case of solid fault ( $R_f = 0 \Omega$ ) the fault location obtained by every method is very accurate. As  $R_f$

**Table 3**

Results of location of ground-fault and calculation of ground-fault resistance for  $x = 8\%$  (top) and  $x = 92\%$  (bottom) (experimental test).

$x$ (%)	$R_f$ ( $\Omega$ )	$V_N$ (V)	$R_{20c}$ ( $\Omega$ )	$x_A^*$ (%)	$x_B^*$ (%)	$R_{fb}^*$ ( $\Omega$ )	$x^*$ (%)	$R_f^*$ ( $\Omega$ )
8	0	18.2	0.3	7.92	7.92	0.3	7.92	0.3
8	20	17.3	19.5	7.51	7.98	20.8	7.98	20.8
8	100	13.9	78.4	6.06	7.93	102.6	7.95	102.7
8	250	9.9	143.7	4.32	7.60	252.7	7.69	254.1
8	500	6.8	199.4	2.94	7.34	497.3	7.53	504.4
8	750	5.0	228.5	2.19	6.97	727.8	7.25	745.5
8	1k	4.0	247.2	1.73	6.70	959.1	7.04	992.8
92	0	210.8	0.2	91.65	91.71	0.2	91.71	0.2
92	20	199.6	18.3	86.77	91.81	19.3	91.82	19.3
92	100	163.3	78.0	71.00	92.73	101.9	93.01	102.1
92	250	120.4	143.2	52.36	91.87	251.3	92.91	252.6
92	500	84.3	199.0	36.65	91.10	494.6	93.49	501.6
92	750	64.7	228.3	28.14	89.54	726.5	93.15	744.2
92	1k	52.2	246.8	22.69	87.61	952.7	92.31	986.0

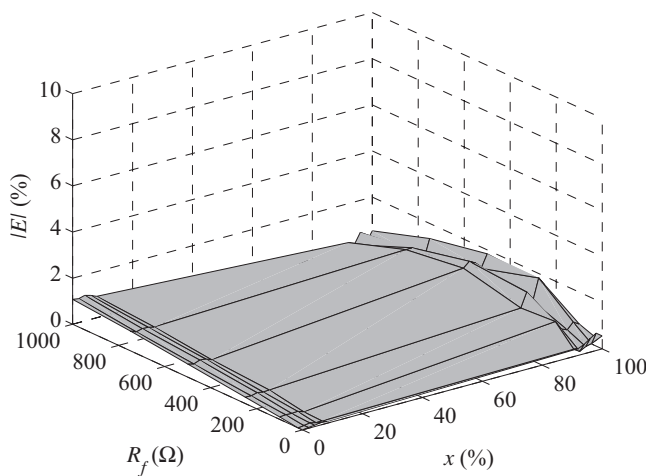


**Fig. 17.** General non-simplified location algorithm (59N + 64S). Absolute value of fault location error  $|E|$  (experimental).

increases from  $0\Omega$  to  $1000\Omega$ , the Simplified Method “A” obtains high error, since the effect of  $R_f$  has a great influence, as described previously. Regarding the Simplified Method “B”, its error increases considerably less than the error by the Simplified Method “A”, and the estimation of the fault resistance,  $R_{JB}^*$  is acceptable. In the case of the general non-simplified location algorithm, the results are once again the best, not only for the fault location  $x^*$ , but also for the fault resistance estimation  $R_f^*$ .

Now, some practical considerations have to be taken into account. Firstly, as expected, the location of the fault in the first 5% of the stator winding is not so accurate. The measurements of  $I_N$  and  $V_N$ , in case of defect in this part of the winding, are affected by the noise and inaccuracy of the measurement, because of its reduced range. The errors in this part of the winding are considerably higher both for  $x_B^*$  and  $x^*$  in the laboratory machine tests, because of its low rated voltage (400 V). However, in this part of the winding, the error of the fault location remains under 2% in both cases, as observed in Fig. 15(b) and in Fig. 17, making the location algorithm acceptable. On the other hand, in synchronous machines of higher rated voltage, the results will improve, because the neutral voltage level, in case of defect in the first part of the winding, will be higher and its measurement will be more precise.

Secondly, the measurement of the low-frequency impedance, for values of  $R_f$  that are close to zero, is not very accurate. This fact is related to the accuracy of the low-frequency injection equipment, and it causes some small error in the fault location, as observed in Fig. 15(b) and in Fig. 17, for  $R_f=0\Omega$ . However, this location error is very low, and the location is still acceptable.

Finally, some aspects need to be pointed out related to the use of the Simplified Method “B” instead of the general non-simplified location algorithm. If possible, the general non-simplified algorithm is always recommended. However, the Simplified Method “B” may be useful for fast location only in generators with especially low value of capacitance-to-ground ( $<0.5\mu\text{F}$ ). It may be more simple to be implemented in a modern protective system. In order to evaluate the error of applying this method for a concrete value of fault resistance, the use of (12) to obtain the value of  $R_{20c}$ , and then the use of (22) to obtain the approximate value of  $E_B$ , is

recommended. If the error does not meet the requirements, then use the general non-simplified method.

## 6. Conclusions

In this paper three methods for on-line ground-fault location in stator windings of synchronous generators has been presented. Firstly, the measurements of neutral voltage or current have been evaluated in order to locate stator-winding ground faults (Simplified Method “A”, 59N), concluding that it is unacceptable as a ground-fault locator. Then, a general on-line location method, based on the measurement of the ground-fault low-frequency injection protection scheme (64S) has been proposed. The main advantages of this algorithm are:

- The stator ground-fault can be located in on-line operating conditions. This method uses the measurements obtained during the protection trip, thus no additional off-line location test would be required.
- No additional equipment is required. This method uses the information provided by the 95% stator ground-fault protection (59N), and the 100% low-frequency injection scheme (64S).
- This method is especially interesting in high-impedance grounded synchronous generators, in which the ground fault cannot visibly be detected, even after the rotor extraction.
- A simplified location algorithm of this method (Simplified Method “B”, 59N + 64S) has been proposed, that is applicable to synchronous generators with especially low capacitance-to-ground, and that may be easier to implement in protective relays.

The general non-simplified ground-fault location algorithm, as well as both simplified methods, has been tested by simulation and laboratory tests for a wide range of fault positions and resistance values. The results obtained are satisfactory, even for a laboratory-scale synchronous machine, in which the location error remains under 5% in any condition for the Simplified Method “B”, and under 2% for the general non-simplified location algorithm. Finally, the positive results obtained in the laboratory, by using this ground-fault location algorithm, assure an interest in future researches on this location method, applied to medium and large power synchronous machines.

## Appendix A.

See Tables A.1 and A.2.

**Table A.1**

Circuit parameters of a real installation for the study of the stator ground-fault location algorithm.

Generator rated voltage	$U_r$	21 kV
Generator rated power	$S_r$	500 MVA
Generator phase voltage	$U_n$	$21/\sqrt{3}\text{ kV}$
Grounding resistance	$R_N$	$1212\Omega$
Total capacitance to ground	$C_T$	$2\mu\text{F}$
Maximum neutral current	$I_{Nmax}$	10 A
Series resistance	$R_s$ (secondary)	$2\Omega$
Series reactance (20 Hz)	$X_s$ (secondary)	$8\Omega$
Injection transformer ratio	$r$	50

**Table A.2**

Circuit parameters and components of the experimental setup for testing the ground-fault location algorithm.

Generator rated voltage	$U_r$	400 V
Generator phase voltage	$U_n$	$400/\sqrt{3}$ V
Grounding resistance	$R_N$	333 Ω
Total capacitance to ground	$C_T$	3 μF
Maximum neutral current	$I_{Nmax}$	0.69 A
Maximum neutral voltage	$V_{Nmax}$	230 V
Series resistance	$R_s$ (secondary)	4.2 Ω
Series reactance (20 Hz)	$X_s$ (secondary)	10.12 Ω
Injection transformer ratio	$r$	16
Equipment	Model	
Protective system	Schneider MiCOM P345	
Low freq. source	Siemens 7XT3300	
Low freq. BPF	Siemens 7XT3400	

## References

- [1] IEEE Guide for AC Generator Protection, IEEE Std C37. 102-2006 (Revision of IEEE Std C37.102-1995), 2006, pp. 1–177.
- [2] IEEE Guide for the Application of Neutral Grounding in Electrical Utility Systems, Part II – Grounding of Synchronous Generator Systems, IEEE Std C62.92. 2-1989.
- [3] M. Fulczyk, J. Bertsch, Ground-fault currents in unit-connected generators with different elements grounding neutral, *IEEE Trans. Energy Convers.* 17 (March (1)) (2002) 61–66.
- [4] L.J. Powell, Stator fault damage considerations for generators on solidly grounded systems, *IEEE Trans. Ind. Appl.* 37 (January/February (1)) (2001) 218–222.
- [5] IEEE Guide for Generator Ground Protection, IEEE Std C37. 101-2006 (Revision of IEEE Std C37.101-1993/Incorporates IEEE Std C37.101-2006/Cor1:2007), (2007 November 15) c1–67.
- [6] IEEE Standard Electrical Power System Device Function Numbers and Contact Designations, IEEE Std C37. 2-1996, 1996.
- [7] M. Fulczyk, Zero-sequence voltages in unit-connected generator for different methods of grounding generator neutral, in: Proc. IEEE DPSP, 2001, pp. 499–502.
- [8] J.W. Pope, A comparison of 100% stator ground fault protection schemes for generator stator windings, *IEEE Trans. Power Appar. Syst. PAS-103* (April (4)) (1984) 832–840.
- [9] C.J. Mozina, 15 years of experience with 100% generator stator ground fault protection – what works, what doesn't and why, in: Proc. IEEE 62nd Annual Conference for Protective Relay Engineers, March 30–April 2, 2009, pp. 92–106.
- [10] R.L. Schlake, G.W. Buckley, G. McPherson, Performance of third harmonic ground fault protection schemes for generator stator windings, *IEEE Trans. Power Appar. Syst. PAS-100* (July (7)) (1981) 3195–3202.
- [11] M. Fulczyk, R. Mydlkowski, Influence of generator load conditions on third-harmonic voltages in generator stator winding, *IEEE Trans. Energy Convers.* 20 (March (1)) (2005) 158–165.
- [12] M. Gilany, O.P. Malik, A.I. Megahed, Generator stator winding protection with 100% enhanced sensitivity, *Electr. Power Energy Syst.* 62 (2002) 167–172.
- [13] G.J. Lloyd, H.T. Yip, G. Millar, Operation, Design and testing of generator 100% stator earth fault protection using low frequency injection, in: Proc. IET DPSP, March 17–20, 2008, pp. 92–97.
- [14] Z. Zhu, Y. Lu, A novel 20 Hz power injection protection scheme for stator ground fault of pumped storage generator, in: Proc. DRPT, April 6–9, 2008, pp. 1911–1915.
- [15] D. Bi, X. Wang, Z. Xu, W. Wang, Analysis and improvement on stator earth-fault protection by injecting 20 Hz signal, in: Proc. IEEE ICEMS 2001, vol. 1, 2001, pp. 301–304.
- [16] T. Nengling, H. Zhijian, Y. Xianggen, L. Xiaohua, Ch. Deshu, Wavelet based ground fault protection scheme for generator stator winding, *Electr. Power Syst. Res.* 62 (2002) 21–28.
- [17] M. Zielichowski, T. Szlezak, Improvements in ground-fault protection of unit-connected generator stator winding using laboratory test environment, *Electr. Power Syst. Res.* 78 (2008) 1635–1639.
- [18] M. Zielichowski, T. Szlezak, A new digital ground-fault protection system for generator-transformer unit, *Electr. Power Syst. Res.* 77 (2007) 1323–1328.
- [19] M. Zielichowski, Third harmonic ground-fault protection system of unit-connected generator with two parallel branches per phase, *Electr. Power Syst. Res.* 78 (2008) 49–57.
- [20] Y.D. Nyanteh, S.K. Srivastava, C.S. Edrington, D.A. Cartes, Application of artificial intelligence to stator winding fault diagnosis in permanent magnet synchronous machines, *Electr. Power Syst. Res.* 103 (2013) 201–213.
- [21] Y. Wang, X. Yin, Z. Zhang, The fault-current-based protection scheme and location algorithm for stator ground fault of a large generator, *IEEE Trans. Energy Convers.* 28 (December (4)) (2013) 871–879.
- [22] C.A. Platero, F. Blázquez, P. Frías, D. Ramírez, Influence of rotor position in FRA response for detection of insulation failures in salient-pole synchronous machines, *IEEE Trans. Energy Convers.* 26 (June (2)) (2011) 671–676.
- [23] Y. Yasa, E. Isen, Y. Sozer, E. Mese, H. Gurleyen, Analysis of doubly fed induction generator wind turbine system during one phase-to-ground fault, in: Proc. IEEE EPE, September 2–6, 2013, pp. 1–8.
- [24] F.R. Blánquez, E. Rebollo, C.A. Platero, Evaluation of the grounding circuit measurements for stator ground-fault location of synchronous generators, in: Proc. IEEE EEEIC, November 1–3, 2013, pp. 229–233.
- [25] X. Zeng, X. Yin, G. Lin, S. Su, D. Chen, Improvement of subharmonic injection schemes for huge hydro-generator stator ground fault protection, in: Proc. IEEE PowerCon, vol. 2, 2002, pp. 707–710.